

A Design on Reduction Cogging Torque of Dual Generator Radial Flux Permanent Magnet Generator for Small Wind Turbine

Gyeong-Chan Lee* and Tae-Uk Jung[†]

Abstract – In this paper, the design for an electromagnetic structure and reduction cogging torque of a dual generator structured RFPM generator, which is a combination of the inner- and outer-rotor types, has been proposed. We call this a dual generator radial flux permanent magnet generator. To reduce the cogging torque, firstly, stator tooth pairing was designed; secondly, stator displacement was designed and finally, stator tooth pairing and stator displacement were carried out simultaneously. We found the optimal design condition about stator tooth pairing angle combination and stator displacement angle for cogging torque minimization. As a result, a cogging was reduced by 93.3[%] by this study.

Keywords: Dual generator, RFPM, Cogging torque, Stator tooth pairing, Stator displacement

1. Introduction

Small scale wind power applications require a cost effective and mechanically simple generator in order to be a reliable energy source. The use of direct driven generators, instead of geared machines, reduces the number of drive components, which offers the opportunity to reduce costs and increases system reliability and efficiency [1].

A small wind turbine using a permanent magnet essentially refer to a RFPM(Radial Flux Permanent Magnet) generator. The RFPM generator, which has a iron core slot in the stator, is easy to manufacture and has a high output voltage and power as well as efficiency. However, because of the existence of iron core slot of the stator, the RFPM generator experiences cogging torque [2].

The cogging torque can bring about an increase in the torque ripple, the vibration and noise generation. It is an important factor to consider for determination of the minimum wind intensity required to generate power in a wind generator [3].

Cogging torque is produced by the interaction between the rotor permanent magnet and the stator teeth. Many methods, such as a fractional number of slots per pole[3], [4], slot skewing [5, 6] magnet skewing [7, 8] auxiliary slots or teeth [3], magnet segmentation [9], pole-arc optimization [3], magnet displacing and shaping [10], etc. have been proposed to reduce the cogging torque [11].

The purpose of this paper is to reduce cogging torque and the design of the electromagnetic structure of the RFPM generator. To reduce the cogging torque, firstly, stator tooth pairing was designed; secondly, stator displacement was designed and finally, stator tooth pairing

and stator displacement were carried out simultaneously. The RFPM generator designed in this study was analyzed by the two-dimensional FEM(Finite Element Method).

2. Design of Dual Generator Radial Flux Permanent Magnet Generator

The RFPM generator is classified into inner-rotor and outer-rotor types.

An inner-rotor type RFPM generator is shown in Fig. 1. The rotor located inside of the stator, thereby having a robust mechanical structure as well as excellent mass-production capability. However, because the rotor is positioned at the inner side where a permanent magnet is attached, its diameter is relatively smaller because of the structural limitation. This limitation causes difficulty in obtaining a high output power because of the relatively small cross-sectional area of the effective output as compared to the total volume, and requires a speed-increasing gear between the generator and a blade because of the low voltage generated at a low speed caused by the

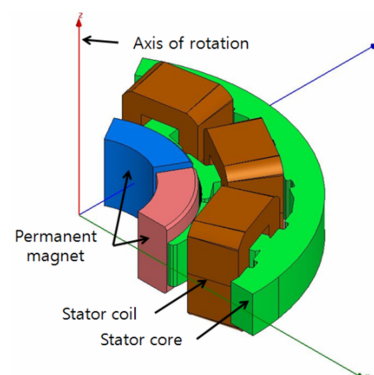


Fig. 1. Inner-rotor type RFPM generator

[†] Corresponding Author : Dept. of Electrical and Electronic Engineering, Kyungnam University, Korea. (tjung@kyungnam.ac.kr)

* Dept. of Electrical and Electronic Engineering, Kyungnam University, Korea. (channy7317@hanma.kr)

Received: September 13; 2013; Accepted: September 24, 2013

lack of a multi-pole structure.

The outer-rotor type RFPM generator is shown in Fig. 2. Since the rotor in this generator is positioned externally thereby creating a bigger effective output power cross-sectional area than that in the inner-rotor structure; this is advantageous in terms of the output power, and low-speed power generation is possible because of the presence of a multi-pole structure. However, in this case, since the inside of the stator is empty, dimensional efficiency is reduced and the cogging torque increases significantly as compared to that in the case of the inner-rotor type RFPM generator.

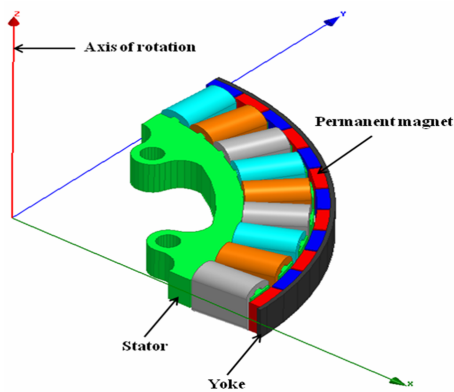


Fig. 2. Outer-rotor type RFPM generator

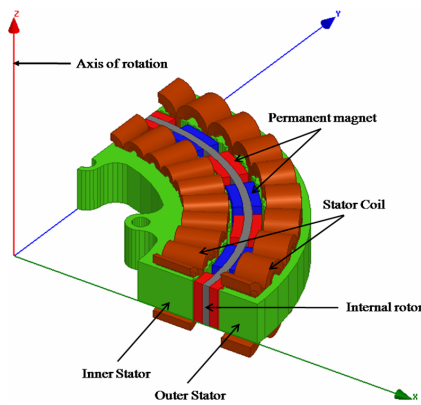


Fig. 3. Shape of proposed DG-RFPMG

Table 1. Specification of DG-RFPMG

Stator	Inner Side	Outer Side
outer diameter[mm]	205	280
inner diameter[mm]	150	243
stack length[mm]	30	30
number of slot	30	30
stator material grade	S60	S60
air-gap[mm]	1	1
coil diameter[mm]	0.912	0.912
coil Turns	94	83
space factor[%]	53.46	53.17
Rotor	Inner Side	Outer Side
outer diameter[mm](PM)	229	241
inner diameter[mm](PM)	207	219
magnet thickness[mm]	6	6
number of pole	20	20
permanent magnet grade	Ferrite 7BE(Br:0.43T)	Ferrite 7BE(Br:0.43T)

In this paper, the design for an electromagnetic structure of a dual generator structured RFPM generator, which is a combination of the inner- and outer-rotor types, has been proposed. We call this a DG-RFPMG(Dual Generator-Radial Flux Permanent Magnet Generator) in this paper.

Fig. 3 shows the shape of the DG-RFPMG. The DG-RFPMG is divided into inner and outer stators for dual generation, and has a rotor to which the permanent magnets positioned between the two stators are attached. Table 1 shows the design specifications of the DG-RFPMG.

3. Cogging Torque

Cogging torque is the oscillatory torque caused by the tendency of the rotor to line up with the stator in a particular direction where the permeance of the magnetic circuit by the magnets is maximized. Cogging torque exists even when there is no stator current. When the PM machines running, additional oscillatory torque components can result from the interaction of the magnet with space-harmonics of the winding layout and with current harmonics in the drive current. These additional oscillatory torque components are electromagnetic and are generally referred to as torque ripple, while the term cogging torque is often reserved for the zero-current condition. In a well designed PM machines the torque ripple and the cogging torque should both be negligible, but it is possible for the torque ripple to exceed the cogging torque by a large amount if the PM machines has an inappropriate combination of winding layout, drive current, and internal geometry [12].

Cogging torque can be reduced by using some minimization technique. Fig. 4 shows the cogging torque minimization technique. The methods of reducing the cogging torque, such as slot skewing and pole-arc to pole-pitch ratio for specific permanent magnet machines, were obtained by the experience, experiments and FEM [11].

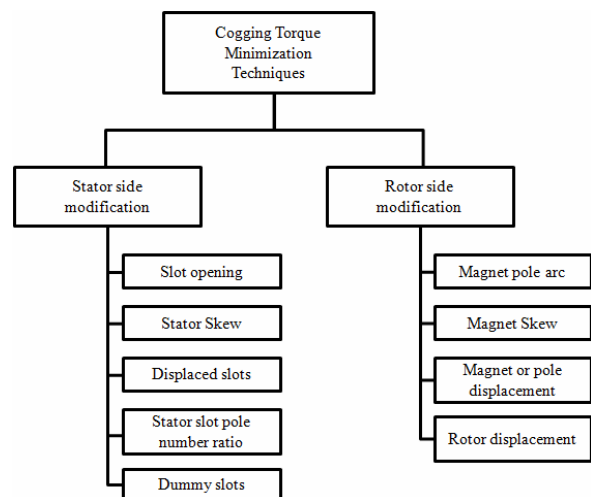


Fig. 4. Summary of cogging torque minimization technique

3.1 Energy method of cogging torque

The cogging torque is the amount of energy variation with respect to the rotation amount of a rotor and can be represented as follows:

$$T = -\frac{\partial W(\alpha)}{\partial \alpha} \quad (1)$$

Where T , $W(\alpha)$, α are the cogging torque, energy in the air-gap, angle of rotor, respectively.

Since the energy variation does not occur substantially except in the air-gap areas, the cogging torque can be obtained by calculating the energy in the air-gap areas. The energy in these areas can be calculated as follows:

$$\begin{aligned} W(\alpha) &= \frac{1}{2\mu_0} \int [G(\theta) \cdot B(\theta, \alpha)]^2 dV \\ &= \frac{1}{2\mu_0} \int_0^{L_s} \int_{R_1}^{R_2} \int_0^{2\pi} G(\theta)^2 \cdot B(\theta, \alpha)^2 d\theta r dr dz \\ &= \frac{1}{2\mu_0} \cdot L_s \cdot \frac{1}{2} (R_2^2 - R_1^2) \int_0^{2\pi} G(\theta)^2 \cdot B(\theta, \alpha)^2 d\theta \end{aligned} \quad (2)$$

Where μ_0 , $G(\theta)$, $B(\theta, \alpha)$, L_s , R_1 , R_2 are permeability of air, relative air-gap permeance function, flux density function, stack length, permanent magnet radius and stator radius, respectively.

The relative air-gap permeance function $G(\theta)^2$ and flux density function $B(\theta, \alpha)^2$ of (2) can be represented by (3) and (4), respectively, using the Fourier series expansion.

$$G(\theta)^2 = \sum_{n=0}^{\infty} G_{nN_s} \cos nN_s \theta \quad (3)$$

$$B(\theta, \alpha)^2 = \sum_{n=0}^{\infty} B_{nN_p} \cos nN_p (\theta + \alpha) \quad (4)$$

Where N_s , N_p are number of slot and number of permanent magnet, respectively.

Therefore, by using (3) and (4) and the orthogonality of the trigonometric function, we can represent (2) as (5):

$$\begin{aligned} W(\alpha) &= \frac{L_s}{4\mu_0} (R_2^2 - R_1^2) \\ &\left[\sum_{n=0}^{\infty} G_{nN_s} B_{nN_p} \int_0^{2\pi} \cos nN_s \theta \cos nN_p (\theta + \alpha) d\theta \right] \\ &= \frac{L_s}{4\mu_0} (R_2^2 - R_1^2) \cdot 2\pi \cdot \sum_0^{\infty} G_{nN_s} B_{nN_p} \cos nN_L \alpha \end{aligned} \quad (5)$$

Where N_L is least common multiple of N_p and N_s .

The cogging torque can be represented by (6) by the partial differentiation of the energy in the air-gap with respect to the rotational angle of a rotor.

$$\begin{aligned} T(\alpha) &= -\frac{\partial W(\alpha)}{\partial \alpha} \\ &= \frac{L_s \pi}{2\mu_0} (R_2^2 - R_1^2) \sum_{n=0}^{\infty} G_{nN_s} B_{nN_p} \sin nN_L \alpha \end{aligned} \quad (6)$$

The cogging torque can be reduced if G_{nN_s} or B_{nN_p} can be assumed to be zero in (6) [11, 13].

4. Cogging Torque Reduction Design

4.1 Stator tooth pairing design

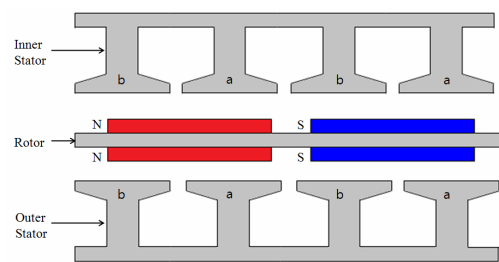
Fig. 5 shows a stator tooth pairing design in which the stator tooth widths a and b are paired.

G_{nN_L} of (6) can be represented by (7) as follows:

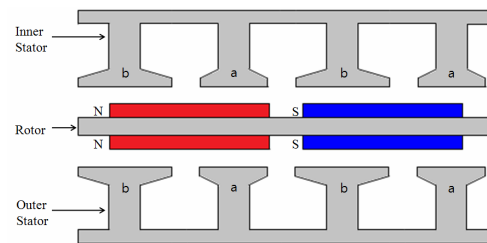
$$\begin{aligned} G_{nN_L} &= \frac{N_s}{\pi} \left(\int_0^{a/2} \cos nN_L \theta d\theta + \int_{2\pi/N_s - b/2}^{2\pi/N_s + b/2} \cos nN_L \theta d\theta \right. \\ &\quad \left. + \int_{4\pi/N_s - a/2}^{4\pi/N_s} \cos nN_L \theta d\theta \right) \\ &= \frac{1}{n\pi} \frac{N_s}{N_L} \left(\sin nN_L \frac{a}{2} + \sin nN_L \frac{b}{2} \right) \end{aligned} \quad (7)$$

By reducing the G_{nN_L} value among values of G_{nN_L} when n is 1, we can eliminate a dominant component of the cogging torque. That is, if a combination of tooth widths a and b that satisfies (8) is found, then a dominant component of the cogging torque can be eliminated [13].

$$\sin nN_L \frac{a}{2} + \sin nN_L \frac{b}{2} = 0 \quad (8)$$



(a) Before stator tooth pairing



(b) After stator tooth pairing

Fig. 5. Stator tooth pairing(tooth widths a and b)

Table 2. Stator tooth pairing widths design

a	b	$\sin N_1 a/2$	$\sin N_1 b/2$	sum
9	9	-1.00	-1.00	-2.00
7.6	10.4	-0.74	-0.74	-1.49
7	11	-0.50	-0.50	-1.00
6.5	11.5	-0.26	-0.26	-0.52

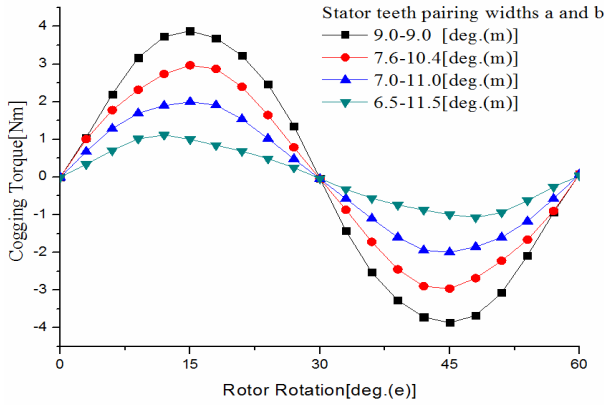


Fig. 6. Cogging torque characteristics according to stator tooth pairing

Table 2 presents the details of the stator tooth pairing design where the stator teeth a and b have the maximum G_{N_L} value and the sum of the design angles a and b is the same for different G_{N_L} values.

Fig. 6 shows one cycle of the cogging torque according to the stator tooth pairing design. The analysis result showed that the smallest cogging torque occurred at the combination of 6.5-11.5[deg.(m)], which has the smallest G_{N_L} value.

4.2 Stator displacement design

The objective of the stator displacement design is to reduce the cogging torque by placing the inner and the outer stators in a staggered pattern as shown in Fig. 7 [14].

The cogging torque generated in the DG-RFPM generator is the sum of the inner and the outer stator and can be represented as follows:

$$\tau_C = \tau_{outer} \sin \theta_C + \tau_{inner} \sin \theta_C \quad (9)$$

Where τ_C , τ_{outer} , τ_{inner} , θ_C are total cogging torque, outer side cogging torque, inner side cogging torque, cogging torque phase, respectively.

The sum of the total cogging torques can be made equal to zero by transitioning the cogging torque phase, which is generated in the outer stator as per (9), by 180 [deg.(e)] as shown in (10).

$$\begin{aligned} \tau_C &= \tau_{Couter} \sin(-\theta_C) + \tau_{Cinner} \sin \theta_C \\ &= -\tau_{Couter} \sin \theta_C + \tau_{Cinner} \sin \theta_C \\ &= 0 \end{aligned} \quad (10)$$

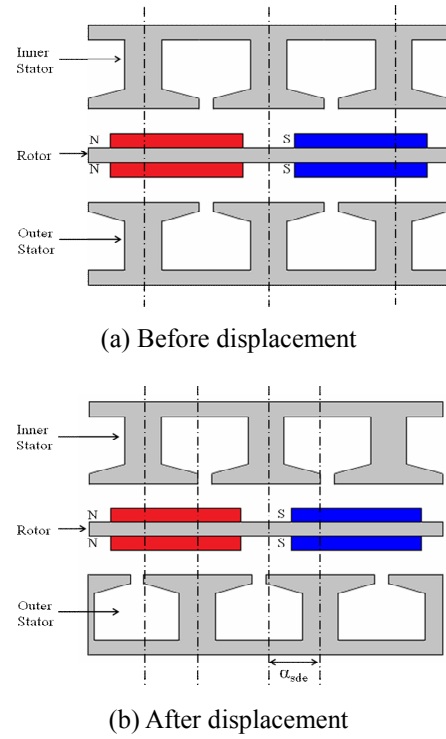


Fig. 7. Definition of stator displacement

N_C denotes the number of occurrences of the cogging torque per rotation in a rotor generated in the inner and the outer stators and can be represented as follows [15]:

$$N_C = \frac{N_p \cdot N_s}{HCF\{N_s, N_p\}} \quad (11)$$

Where $HCF\{N_s, N_p\}$ is the highest common factor of the number of slot and number of permanent magnet.

Therefore, the mechanical angle at which the cogging torque occurs once is as follows:

$$\alpha_C = \frac{360^\circ}{N_C} [\text{deg.}(m)] \quad (12)$$

Then, by expressing this as an electrical angle, we obtain the following:

$$\alpha_{Ce} = \frac{P}{2} \alpha_C [\text{deg.}(e)] \quad (13)$$

Therefore, the stator displacement transition angle to move the cogging torque phase by 180[deg.(e)], which is generated in the outer stator, can be represented as follows:

$$\begin{aligned} \alpha_{sde} &= \frac{1}{2} \cdot \alpha_{Ce} \\ &= \frac{1}{2} \cdot \frac{P}{2} \cdot \alpha_C \end{aligned} \quad (14)$$

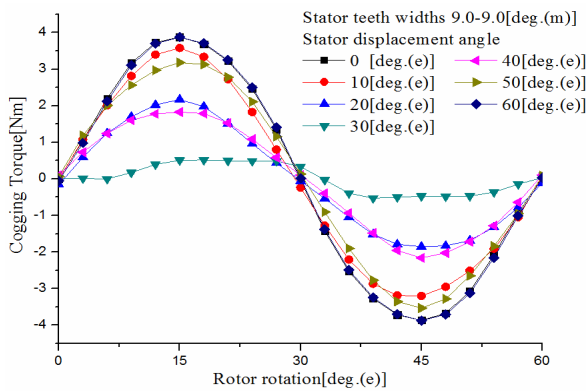


Fig. 8. Cogging torque characteristics according to stator displacement

$$= \frac{1}{2} \cdot \frac{p}{2} \cdot \frac{360^\circ}{N_c}$$

$$= 90^\circ \cdot \frac{HCF\{N_s, P\}}{N_s} [\text{deg.}(e)]$$

Fig. 8 shows one cycle of the cogging torque according to the stator displacement design. At the initial 0[°], a cogging torque of 3.88[Nm] was generated. While displacing the stator, we observed that the cogging torque was reduced by 86.6[%] to 0.52[Nm] when the stator location was moved by 30 [deg.(e)].

5. Stator Tooth Pairing and Displacement Combination Design

The combined design optimization was considering to reduce the cogging torque. Fig. 9 shows two-dimensional FEM model of DG-RFPMG which has designed both the stator tooth pairing and the stator displacement.

Fig. 10 show the distribution curve of the maximum cogging torque for different angles when the stator tooth pairing and the stator displacement design are applied

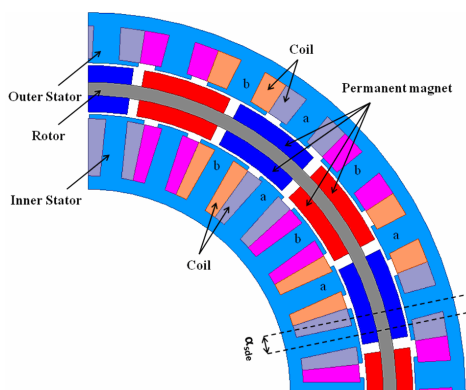


Fig. 9. Two-dimensional FEM model of DG-RFPMG(1/4 model)

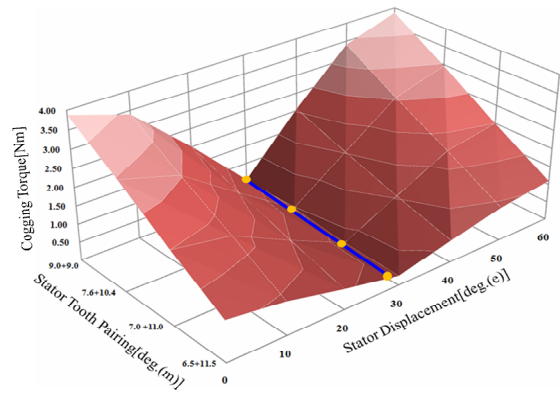


Fig. 10. Distribution curve of the maximum cogging torque

Table 3. Analysis results of cogging torque according to combination design

Displacement Pairing	0	10	20	30	40	50	60
9.0+9.0	3.88	3.4	2.02	0.52	2.05	3.4	3.87
7.6+10.4	2.97	2.53	1.48	0.48	1.52	2.54	2.97
7.0+11.0	2	1.74	1	0.31	1.03	1.75	2
6.5+11.5	1.12	0.91	0.56	0.26	0.6	0.91	1.1

Cogging torque unit : [Nm]

simultaneously. And Table 3 shows analysis results of cogging torque. The analysis results shows that the minimum cogging torque was 0.26[Nm], which was observed at the stator tooth pairing of 6.5-11.5[deg.(m)] and stator displacement of 30[deg.(e)].

6. Conclusion

In this paper, we proposed the design of electromagnetic structure of DG-RFPMG and cogging torque reduction. To reduce the cogging torque, a stator tooth pairing and stator displacement design was applied. We found the optimal design condition about stator tooth pairing angle combination and stator displacement angle for cogging torque minimization. As a result, a cogging was reduced by 93.3[%] by this study.

References

- [1] A. P. Ferreira, A. M. Silva, A. F. Costa, "Prototype of an Axial Flux Permanent Magnet Generator for Wind Energy Systems Applications" *Power Electronics and Applications*, 2007 European Conference, pp. 1-9, Sept. 2007.
- [2] K. S., R. Krishnan, "Performance Comparisons of Radial and Axial Field, Permanent-Magnet, Brushless Machines", in *Proceedings of IEEE Industry Applications*, vol. 37, no. 5. pp. 1219-1226, sept. 2001.
- [3] Z.Q. Zhu, David Howe, "Influence of Design

Parameters on Cogging Torque in Permanent Magnet Machines” *IEEE transactions energy con-version*, vol. 15, no. 4, December 2000.

- [4] C. C. Hwang, S. B. John, and S. S. Wu, “Reduction of cogging torque in spindle motors,” *IEEE Trans. Magn.*, vol. 34, no. 2, pp. 468-470, Mar. 1998.
- [5] D. C. Hanselman, “Effect of skew, pole count and slot count on brushless motor radial force, cogging torque and back EMF,” *Proc. Inst. Elect. Eng.*, vol. 144, no. 5, pp. 325-330, 1997.
- [6] S. M. Hwang, J. B. Eom, Y. H. Jung, D. W. Lee, and B. S. Kang, “Various design techniques to reduce cogging torque by controlling energy variation in permanent magnet motors,” *IEEE Trans. Magn.*, vol. 37, no. 4, pp. 2806-2809, Jul. 2001.
- [7] N. Bianchi and S. Bolognani, “Design techniques for reducing the cogging torque in surface-mounted PM motors,” *IEEE Trans. Ind. Appl.*, vol. 38, no. 5, pp. 1259-1265, 2002.
- [8] M. Lukaniszyn, M. Jagiela, and R. Wrobel, “Optimization of permanent magnet shape for minimum cogging torque using a genetic algorithm,” *IEEE Trans. Magn.*, vol. 40, no. 2, pp. 1228-1231, Mar. 2004.
- [9] R. Lateb, N. Takorabet, and F. Meibody-Tabar, “Effect of magnet segmentation on the cogging torque in surface-mounted permanent-magnet motors,” *IEEE Trans. Magn.*, vol. 42, no. 3, pp. 442-445, Mar. 2006.
- [10] A. Keyhani, C. Studer, T. Sebastian, and S. K. Murth, “Study of cogging torque in permanent magnet motors,” *Elect. Mach. Power Syst.*, vol. 27, no. 7, pp. 665-678, Jul. 1999.
- [11] Li Zhu, S.Z. Jiang, Z. Q. Zhu, C. C. Chan, “Analytical Methods for Minimizing Cogging Torque in Permanent-Magnet Machines”, *IEEE Transactions on Magnetism*, Vol. 45, No. 4, April 2009
- [12] J. R. Hendershot Jr., TJE Miller, “Design of Brushless Permanent-Magnet Motors”, *Magn and Clarendon press, Oxford*, 1994.
- [13] Sang-Moon Hwang, Jae-Boo Eom, Geun-Bae Hwang, Weui-Bong Jeong and Yoon-Ho Jung, “Cogging Torque and Acoustic Noise Reduction in Permanent Magnet Motors by Teeth Pairing” in *Proceedings of IEEE transactions on magnetism*, vol. 36, no. 5, september 2000.
- [14] Alvaro B. Letelier, Delvis A. Gonzalez, Juan A. Tapia, “Cogging Torque reduction in an axial flux pm machine via stator slot displacement and skewing”, *IEEE transactions on industry applications*, vol. 43, no. 3, May/June 2007
- [15] P. Sivachandran, P. Venkatesh, N. Kamaraj, “Cogging Torque Reduction in Dual-Rotor Permanent Magnet Generator for Direct Coupled Stand-Alone Wind Energy Systems” *IEEE International Conference on, Sustainable Energy Technologies*, 2008



Gyeong-Chan Lee He received B.S and M.S degree in electrical engineering from Kyungnam University. He is currently a Ph. D. student at Kyungnam University. His research interests are design and analysis of motor and generator.



Tae-Uk Jung He received B.S, M.S and Ph.D. degree in electrical engineering from Pusan national university. He is currently a Professor at Kyungnam University. His research interests are modeling of electrical machines and devices.